Influence of dynamic strain ageing on damage in austenitic stainless steels

Mattias Calmunger[1,a], Guocai Chai[1,2,b], Sten Johansson[1,c] and Johan Moverare[1,d]

[1] Division of Engineering Materials, Department of Management and Engineering, Linköping University, SE-58183 Linköping, Sweden

[2] AB Sandvik Material Technology R&D center, SE-81181 Sandviken, Sweden

[a]mattias.calmunger@liu.se, [b]guocai.chai@sandvik.com, [c]sten.johansson@liu.se, [d]johan.moverare@liu.se

Keywords: Dynamic strain ageing, biomass power plant, austenitic stainless steel, twins, damage.

Abstract. Dynamic strain ageing (DSA) phenomena in five austenitic materials (three austenitic steels and two nickel alloys) have been investigated by tensile testing at temperatures up to 700°C. The deformation and damage behaviours are investigated using electron channeling contrast imaging (ECCI) and electron backscattering diffraction (EBSD). Dynamic strain ageing behaviour varies greatly with alloy composition and temperatures. The results from this study show that DSA is not always related to reduction of ductility or embrittlement, in fact the ductility in some materials can increase in the DSA regime. This is attributed to the formation of nano twins by DSA stimulated twin induced plasticity (TWIP). Micro damage mechanisms due to DSA were also investigated. Damage due to interactions between slip bands and interaction between twins in grains or at grain boundaries are observed and discussed.

Introduction

Austenitic stainless steels are commonly used as structural material in biomass power plants. Renewable energy resources with high efficiency are highly desired for sustainable energy production. Increased efficiency in biomass power plants requires higher temperature and pressure. However, the materials used for biomass power plants with higher temperature and pressure also need to be resistant to the corrosive atmosphere connected to combustion of biomass fuel [1].

Austenitic stainless steels show dynamic strain ageing (DSA) in a wide range of temperatures from 200 to 800°C [2-5], which involves the operating temperature range of biomass power plants. The phenomenon DSA is an interaction between solute atoms and moving dislocations during plastic deformation. It is influenced by temperature and strain rate which directly influence the mobility of dislocations and diffusing solute atoms [3,6-8]. In austenitic stainless steels the responsible elements for DSA are interstitials such as carbon and nitrogen. At temperatures below 350°C carbon is responsible for the DSA while nitrogen and/or substitutional chromium atoms are responsible at higher temperatures (400°C to 650°C). It has been reported that mechanical properties like strength and ductility may be significantly changed due to DSA [9,10]. DSA is characterized by serrated yielding occurring in the stress-strain curve, denoted as Portevin-Le Châtelier (PLC) effect. The PLC effect is due to the pinning and unpinning of dislocations or formation of new dislocations. The solute atom pinning of dislocations will raise the stress until they are released (unpinned) or new dislocations are formed which will result in an instant relaxation of stress [2,6-9].

Damage related to DSA in austenitic stainless steels have been investigated in several ways, as thermo-mechanical fatigue (TMF), creep [11] and low-cycle fatigue (LCF) [9,12,13]. Bae et al. [11] reported that creep and DSA are both active in the TMF test temperature ranges 400°C-650°C and 450°C-700°C with different cycle conditions. However, according to Bae et al. the dominant damage mechanism varies between the test conditions. Creep is dominant in the temperature range 450°C-700°C. Creep is also responsible for the minimum TMF life in the counter-clockwise-diamond condition for the temperature range 400°C-650°C where most of the damage was found. In a study by Hong et al. [12] it was shown that DSA can reduce crack initiation time as well as crack propagation life in LCF tests. DSA induce inhomogeneous deformation resulting in multiple crack initiation and will therefore reduce the crack initiation time. DSA induced hardening is also responsible for increase in crack propagation rate [12]. The reduction in fatigue life becomes more damaging with decreasing strain rate than with an increase in temperature. This is due to higher amount of hardening induced by DSA [14]. In the case of LCF, cracks typically initiates in grain and twin boundaries, from inclusions and most often in persistent slip bands [15].

This study was focused on damage mechanisms related to DSA in three austenitic stainless steels and two nickel-base alloys. The materials were investigated by tensile testing at different temperatures (400°C to 700°C) and LCF testing at 650°C with a strain range of 1,2%. Since DSA is present in different temperature ranges depending on alloy composition, a scanning electron microscope (SEM) investigation is made at 650°C where all five materials displayed DSA.

Experimental Procedures

Materials. Three austenitic stainless steels, Sanicro 25, AISI 310 and AISI 316L and two nickel-base alloys, Alloy 617 and Alloy 800HT were used in this study. Both types were solution treated before testing. Table 1 shows the chemical composition of the five materials.

Table 1. Nominal composition of the investigated materials in wt%.

Material	C	Si	Mn	Cr	Ni	W	Co	Cu	Nb	N	Mo	Fe
Sanicro 25	0.1	0.2	0.5	22.5	25	3.6	1.5	3.0	0.5	0.23	-	Bal.
AISI 310	0.045	0.55	0.84	25.4	19.2	-	-	0.08	-	-	0.11	Bal.
AISI 316L	0.04	0.4	1.7	17	12	-	-	-	-	-	2.6	Bal.
Alloy 617	0.1	-	-	22.5	53.8	-	12	-	-	0.5	9	1.1
Alloy 800HT	0.07	0.6	0.6	20.5	30.5	Al/0.5	Ti/0.5	-	-	-	-	Bal.

Tensile deformation. First of all the DSA must be obtained which is done by tensile testing, obtaining stress-strain curves showing serrated yielding. For this a Roell-Korthaus tensile test machine was employed, equipped with a MTS 653 furnace and Magtec PMA-12/2/VV7-1 extensometer in air environment. Round-bar specimens with 5 mm in diameter and 50 mm gauge length were used. The tensile test were carried out at a strain rate of $2*10^{-3}s^{-1}$. Six temperatures were used, room temperature (RT) as reference and 400°C, 500°C, 600°C, 650°C and 700°C for obtaining DSA.

Low cycle fatigue. In this investigation LCF properties were obtained using a push-pull mode and a frequency of 0.05 Hz. A cylindrical specimen 10 mm in diameter and a gauge length for strain measurement of 12.5 mm was used. Only Sanicro 25 was used in the LCF tests and was subjected to strain amplitude of 0.6% at 650°C.

Scanning electron microscopy investigation. An OXFORD electron backscatter diffraction (EBSD) system with HKL software attached to a HITACHI SU-70 FEG-SEM were employed for the EBSD analysis. The cross-section parallel to the loading axis in all the materials subjected to tensile test to fracture at RT and 650°C was polished carefully. This investigation produced orientations of particular grains in the microstructure and misorientation profiles. In order to investigate damage mechanisms for tensile tested fractured specimens and the LCF specimen, the electron channelling contrast imaging (ECCI) technology was used. This was done on the fractured tensile specimens, tested at the temperatures RT and 650°C.

Results

Dynamic strain ageing behaviours in the austenitic stainless steels. Fig. 1 and 2 shows the mechanical behaviour of four austenitic materials during the tensile testing at RT, 600°C and 650°C. Serrated yielding can be observed in all materials at higher temperatures (400°C to 700°C). All materials show a marked decrease in yield strength at high temperature compared to room temperature but different behaviour in the strain after fracture. AISI 316L shows a continuous decrease of ductility with increasing temperature. This can also be observed in AISI 310 material. Sanicro 25 and Alloy 800HT have an increase in ductility with increased temperature up to 600°C, but then the ductility decreases with further increase in temperature. Nickel base alloy 617 shows a continuous increase in ductility with increasing temperature.

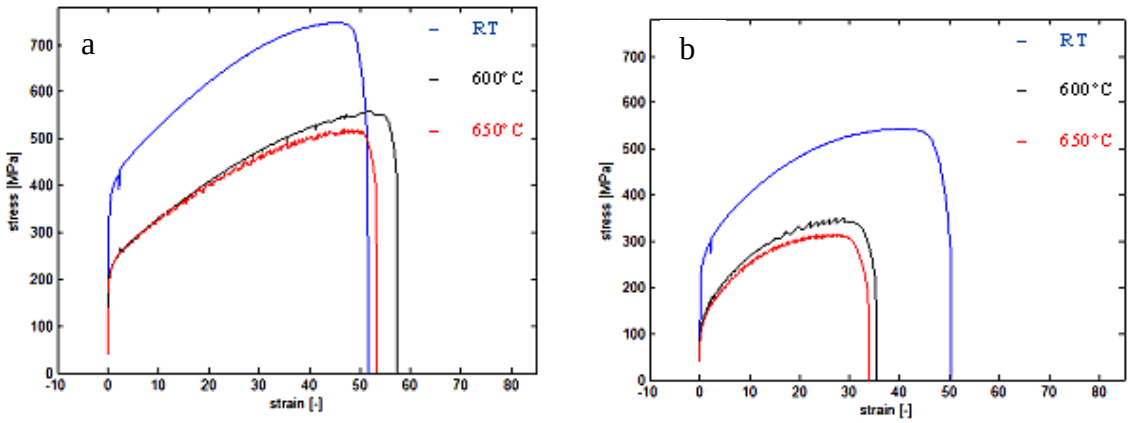

Fig. 1. Engineering stress-strain curves display RT and elevated temperatures, a) Sanicro 25, b) AISI 316L.

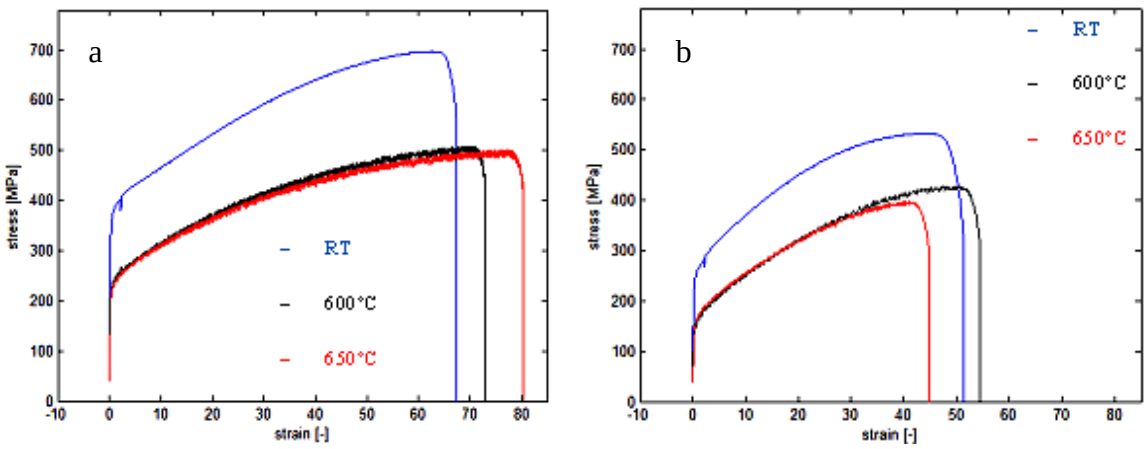

Fig.2. Engineering stress-strain curves display RT and elevated temperatures, a). Alloy 617, b). Alloy 800HT.

Influence of dynamic strain ageing on deformation damage. Fig. 3 shows the deformation and damage behaviour of AISI 310 during the tensile testing. At room temperature (RT) large deformation bands (DB) or slip bands and interaction between slip bands are typical damage phenomena. Localized damage appears where multi-direction planar slip bands intersect with each other (Fig. 3a). At high temperature or dynamic strain ageing regime, twins can also be seen in the tested material. The damage occurs often at interaction between twins and grain boundaries (GB). Planar slip is creating highly plastically deformed zones where interaction with grain boundaries takes place (Fig. 3b and c).

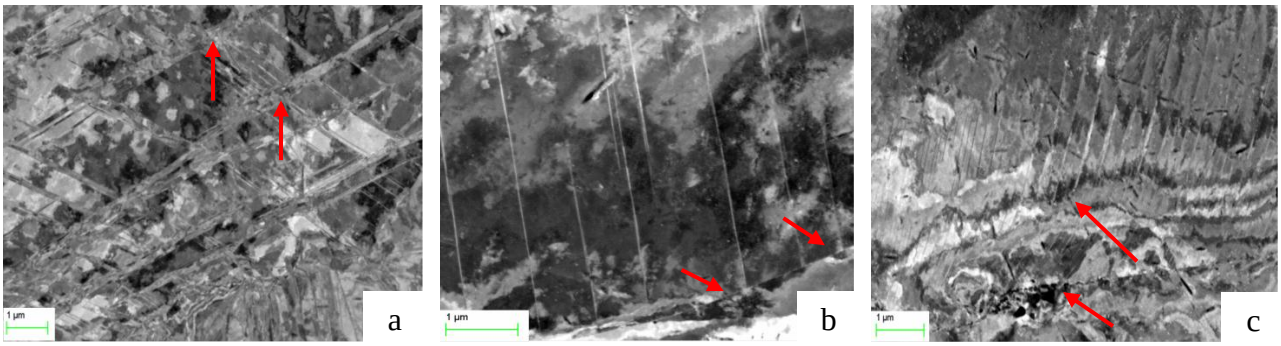

Fig. 3. Deformation and damage behaviour of AISI 310 during the tensile testing, a). At RT, formation and interaction of DB, b). At 600°C, interaction of twins and GB, c). at 650°C, interaction of twin or DB and GB.

Damage behaviour in different materials. Fig. 4 shows the damage behaviour of different austenitic materials. In Fig 4a or AISI 316L material, several deformation bands (DB) or shear bands can be found. In these bands, very small grains or subcells can be observed. They look like recrystallization microstructure (Fig. 4d). These small grain or subcells are less than 1 μm in diameter. In Fig. 4b (Sanicro 25) and 4c (Alloy 617), there are several large deformation bands. No small subcell can be observed. Actually, they contain many small deformation bands (Fig. 4f). Between two large DBs, there are several small bands. They can probably be multi twinning in different crystallographic orientations. Damage can be observed at the interactions between large DB and small bands. Even at interactions between twins, damage can be observed (Fig. 4e). The

interaction between large DB and grain boundaries can usually cause formation of micro cracks (Fig. 4f).

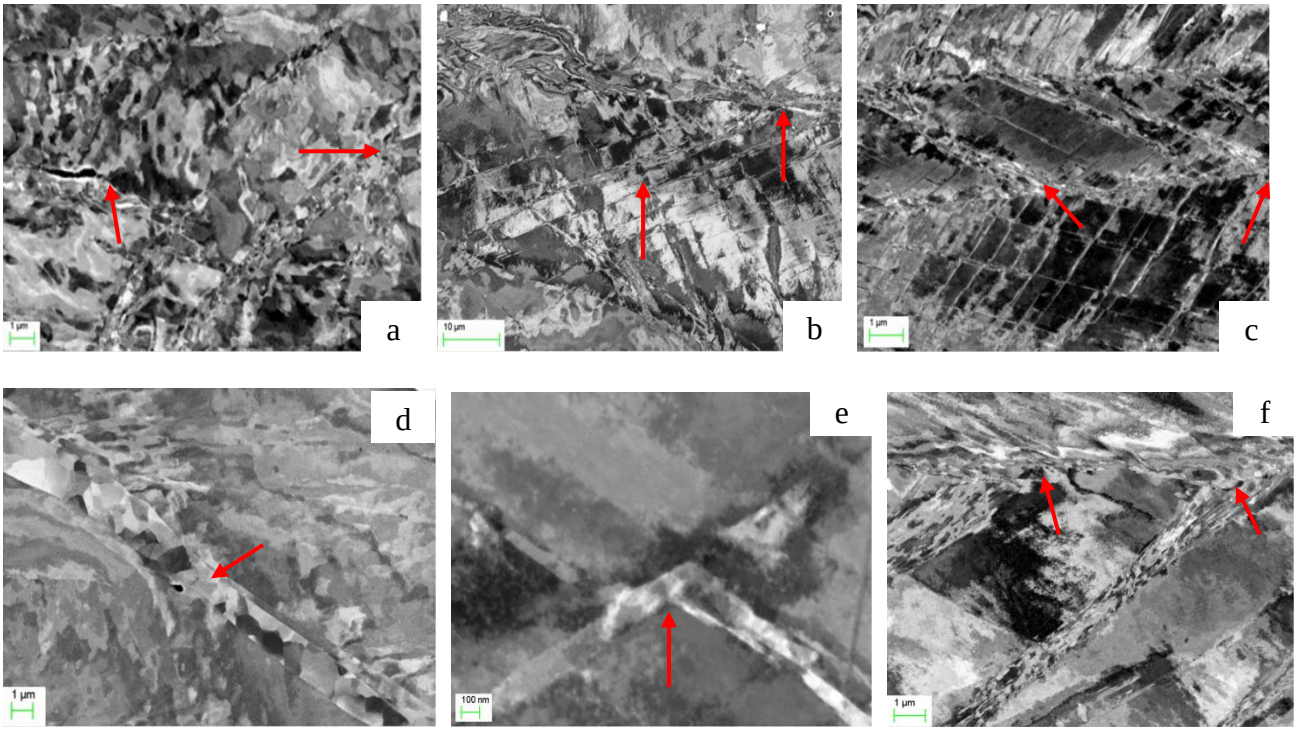

Fig.4. Deformation and damage behaviours by ECCI in: a) and d). AISI 316L, formation of large DB and small subcells, b) and e). Sanicro 25, formation of large DB and localized damage due to intersection between twins, c) and f). Nickel base alloy 617, interactions between DB and GB and twins and DB. All materials tensile tested at 650°C.

Similar damage as for the tensile tested materials was found in the microstructure of LCF tested Sanicro 25 at 650°C, also showing DSA. Planar deformation slip bands create damage or even crack initiation when they interact with grain boundaries, as shown in Fig. 5.

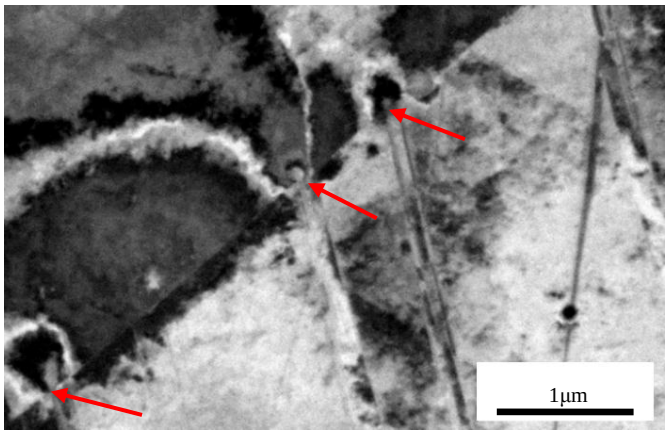

Fig.5. ECCI picture display LCF tested Sanicro 25 at 650°C, strain range 1,2% and 1571 cycles, showing damage or crack initiation sites due to intersection between slip bands and grain boundary. Red arrows are pointing out damage.

Discussion

Since dynamic strain ageing is an interaction between solute atoms and moving dislocations during plastic deformation, it is considered to decrease the ductility of the material. In this test, however, some alloys show an increase in ductility during DSA. One possible explanation for this is the formation of twins during DSA. When dislocation movement is stopped or restricted by solute atoms during DSA, deformation can occur by twinning in some material. As known, formation of each twin leads to a certain shear strain. This will increase plasticity of the material if plenty of twins have been formed, which is called twin induced plasticity (TWIP) [16]. Fig. 6 shows the nano twins formed in some of the materials during DSA. Formation of these nano twins may lead to an increase in ductility as shown in Fig. 1 and 2.

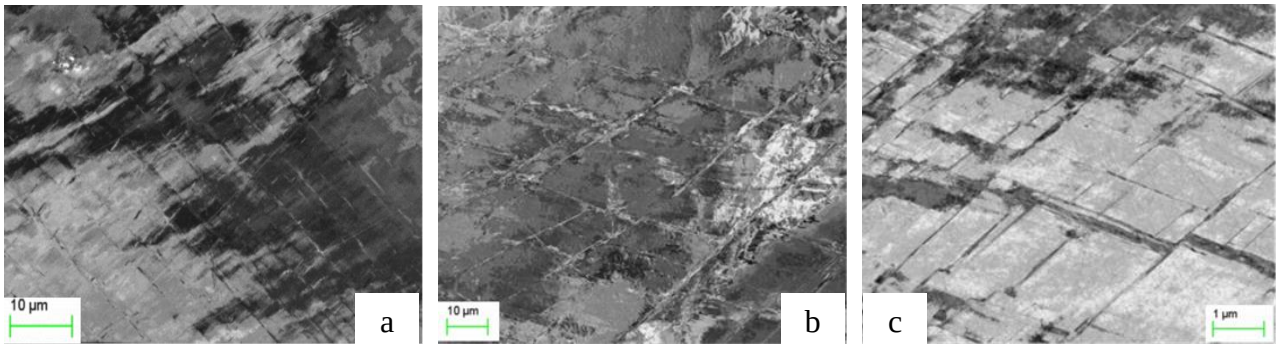

Fig. 6. ECCI pictures show formation of twins, a). in Sanicro 25, in one crystallographic direction, b). in Alloy 800HT in multi crystallographic directions, c). in Alloy 617, in multi crystallographic directions. All materials tensile tested at 650°C.

The formation of twins during DSA is confirmed by the EBSD map in Fig. 7. The crystallographic orientation is displayed according to the coloured stereographic triangle to the right. The misorientation profiles in Fig. 7 show variations in orientation along the directions pointed out by the two arrows (X and Y). An angular difference of 60° indicates twin boundaries, shown by arrow (X). Along the path indicated by arrow (Y) a more continuous increase in misorientation indicates dislocation activity like planar slip and slip bands or cell structure. Cell structure has only been seen in the tensile test specimens at RT. The twins and slip bands are almost perpendicular to each other which indicate that orientation relative to the load direction influence the formation of twins. The {111}-orientations that are blue in Fig. 7 have a lower Schmidt factor (SF) than the others, also the grains close to that orientation show lower degree of plastic deformation. The SF is also influencing the formation of twins, a lower SF orientation seems to be more likely to form twins rather than higher SF orientations. The amount of twins is decreasing with higher temperature, as reported by others [17,18]. However, twins appear in some of the five materials despite the high temperature and can probably be initiated by the instant higher local stress peaks caused by the DSA process. This can cause similar effects as TWIP and probably be related to the improved effect of ductility.

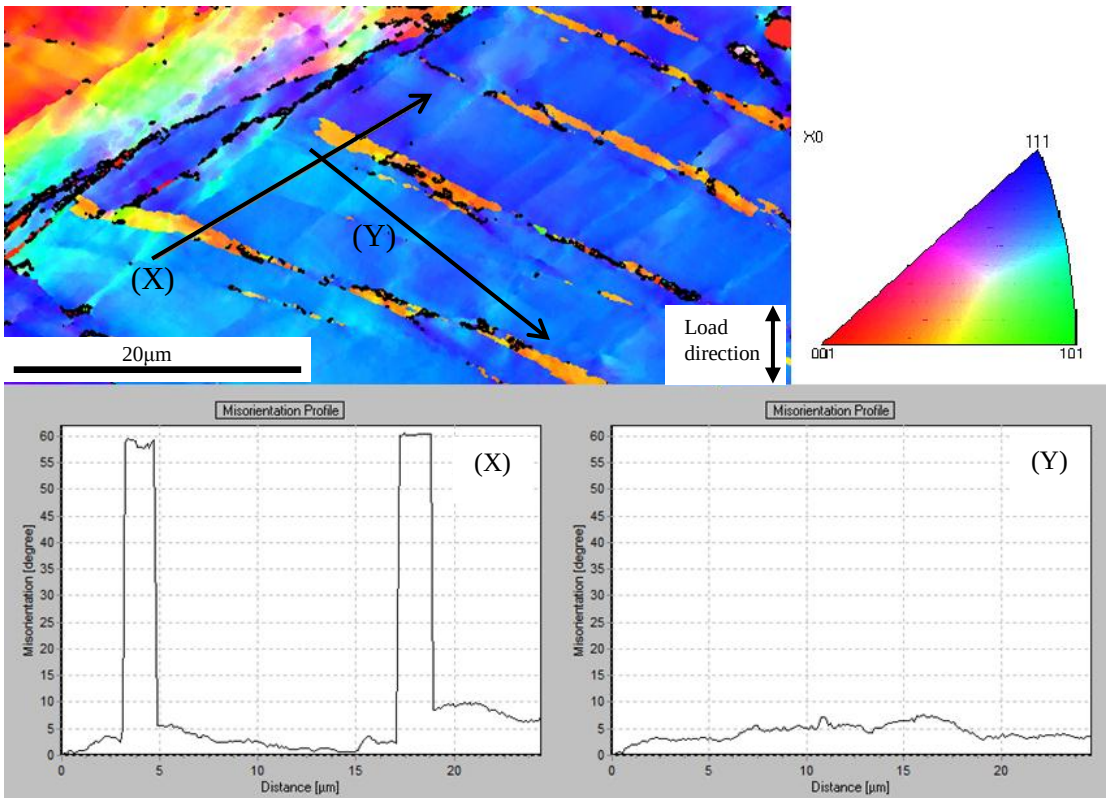

Fig. 7. EBSD analysis displaying orientation and misorientation profiles showing twins with angle 60° (X) and low angle deformation (Y) in Sanicro 25 at 650°C.

DSA is present in all five material but at different temperature ranges. As expected deformation in the DSA regimes is planar [9], i.e. slip bands in multi-directions and planar slip. This type of deformation creates localized stress concentration and damage when the slip bands or damage bands interact with grain boundaries or each other. Also planar slip is causing damage zones as a result of the dislocations active in the grain boundary area, as shown in Fig. 3 and 4. At RT, damage occurs mainly at large DB or interactions between DB and grain boundary. At high temperature, besides the above mechanism, damage due to twins interacting with DB and GB or each others can also be a possible damage mechanism.

Formation of small subcells in highly strained deformation bands in AISI 316L during tensile test at high temperature can be the origin of recrystallization. This may be due to high stacking fault energy (SFE) that causes the formation of dislocation subcells with a heavy plastic deformation at a certain temperature [19]. The upper and lower limits for recrystallization and formation of twins are thus dependent on the deformation and temperature pre history in those alloys.

Conclusions

Tensile testing of five austenitic materials at room temperature, 400ºC to 700ºC, LCF testing at 650°C and subsequent study of microstructure by ECCI and EBSD has led to the following conclusion.

- DSA is present in all five austenitic materials and influences the deformation mechanism.
- Local damage has been connected to interaction between slip bands and/or interaction between twins and grain boundaries.
- Total strain at fracture is affected differently by temperature depending on alloy tested.
- Damaged areas with high local plasticity show recrystallization.
- Deformation twins are created during deformation at high temperature.

Acknowledgements

Present study was financially supported by AB Sandvik Material Technology in Sweden and the Swedish National Energy Administration through the Research Consortium of Materials Technology for Thermal Energy Processes, Grant No. KME-501. The assistance work with the ECCI pictures by Mr Jerry Lindqvist is appreciated.

References

[1] Pettersson J, Asteman H, Svensson J, Johansson L. Oxidation of Metals, Vol 6 (2005), p.23.
[2] de Almeida LH, Emygdio PRO, Le May I. Scripta Metallurgica et Materialia, Vol. 31 (1994), p.505.
[3] de Almeida LH, Le May I, Emygdio PRO. Mater Charact, Vol. 41 (1998), p.137.
[4] Samuel KG, Mannan SL, Rodriguez P. Acta Metallurgica, Vol. 36 (1988), p.2323.
[5] Karlsen W, Ivanchenko M, Ehrnstén U, Yagodzinskyy Y, Hänninen H. J Nucl Mater, Vol. 395 (2009), p.156.
[6] Van Den Beukel A. Acta Metallurgica, Vol. 28 (1980), p.965.
[7] Sleeswyk AW. Acta Metallurgica, Vol. 6 (1958), p.598.
[8] Mulford RA, Kocks UF. Acta Metallurgica, Vol. 27 (1979), p.1125.
[9] Hong S, Lee S. J Nucl Mater, Vol. 340 (2005), p.307.
[10] Mannan SL, Samuel KG, Rodriguez P. Materials Science and Engineering, Vol. 68 (1985), p.143.
[11] Bae K, Kim H, Lee S. Materials Science and Engineering: A, Vol. 529 (2011), p.417.
[12] Hong S, Lee K, Lee S. Int J Fatigue, Vol. 27 (2005), p.1420.
[13] Prasad Reddy GV, Sandhya R, Bhanu Sankara Rao K, Sankaran S. Procedia Engineering, Vol. 2 (2010), p.2181.
[14] Rodriguez P. Bulletin of Materials Science, Vol. 6 (1984), p.653.
[15] Mu P, Aubin V. Procedia Engineering, Vol. 2 (2010), p.1951.
[16] Grässel O, Krüger L, Frommeyer G, Meyer LW. Int.J.Plast, Vol. 16 (2000), p.1391.
[17] Wu X, Pan X, Mabon JC, Li M, Stubbins JF. J Nucl Mater, Vol. 356 (2006), p.70.
[18] Meyers MA, Vöhringer O, Lubarda VA. Acta Materialia, Vol. 49 (2001), p.4025.
[19] Curtze S, Kuokkala V. Acta Materialia, Vol. 58 (2010), p.5129.